The impact of precipitating ice and snow on the radiation balance in global climate models

D. E. Waliser,[1] J.-L. F. Li,[1] T. S. L'Ecuyer,[2] and W.-T. Chen[1]

Received 15 December 2010; revised 1 February 2011; accepted 9 February 2011; published 23 March 2011.

[1] Climate models often ignore the radiative impact of precipitating hydrometeors. CloudSat retrievals provide the first means to distinguish between cloud versus precipitating ice mass and characterize its vertical structure. With this information, radiative transfer calculations are performed to examine the impact of excluding precipitating ice on atmospheric radiative fluxes and heating rates. The preliminary results show that such exclusion can result in underestimates of the reflective shortwave flux at the top of the atmosphere (TOA) and overestimates of the downwelling surface shortwave and emitted TOA longwave flux, with the differences being about 5–10 Wm^{-2} in the most convective and rainfall intensive areas and greatest for the TOA longwave flux. There are also considerable differences (~10–25%) in the vertical profiles of shortwave and longwave heating, resulting in an overestimation (~up to 10%) of the integrated column cooling. The implications of these results are that models that exclude these ice components are achieving TOA radiation balance through compensating errors as well as possibly introducing biases in atmospheric circulations. **Citation:** Waliser, D. E., J.-L. F. Li, T. S. L'Ecuyer, and W.-T. Chen (2011), The impact of precipitating ice and snow on the radiation balance in global climate models, *Geophys. Res. Lett.*, *38*, L06802, doi:10.1029/2010GL046478.

1. Introduction

[2] One of the most groundbreaking observations to arrive with the development of the A-Train [*Stephens et al.*, 2002] for the purposes of understanding and better modeling clouds and convection is the cloud-radar reflectively measurements from CloudSat that provide for the retrieval of cloud ice and liquid water profiles [*Stephens et al.*, 2008]. These estimates have been sorely needed for model development and evaluation as the variations in the annual mean integrated ice water path (IWP) and liquid water path (LWP) between global climate models (GCMs) contributing to the IPCC AR4 range over two orders of magnitude [*Li et al.*, 2008; *Waliser et al.*, 2009]. Key to the proper use of satellite retrievals in the evaluation of modeled cloud ice and liquid is that many GCM representations ignore or diagnostically treat the falling hydrometeor components (e.g., rain, snow) and only consider – for the purposes of radiation calculations – the "suspended" component of water that the model deems "clouds".

[3] The rationale for this is that the areas of the precipitating elements are so small and infrequent that their impact on radiation is small and that the precipitating hydrometeors in these precipitating areas are large enough that they have very little impact on cloud radiative properties. For example, most of the GCMs contributions to AR4 such as the CGCM3.1, ECHAM5, FGOALS-g1.0, INGV-SXG, and INM-CM3.0 only include cloud ice from stratiform clouds and ignore the ice in convective cores, convective-anvils and in the precipitation. The GISS contributions to AR4 do include contributions from convective core in addition to stratiform cloud ice using a very simple construct related to the pressure thickness of the clouds, but the model still ignores the precipitating ice. The CSIRO GCM includes a single prognostic variable that represents both cloud ice and precipitating ice in the stratiform cloud scheme for radiation but ignore the contributions from the anvil and convective cores. Other models such as the NASA GEOS5, ECMWF IFS, and NCEP's GFS and CFS, which do have climate time scale applications, include the effects of cloud ice from stratiform clouds and convective detrained anvils but ignore the contributions from convective cores and precipitating snow. While the exclusions discussed above are sound to first order, we now have global satellite observations that suggest that the amount of precipitating ice is on the order of 2/3 of the total ice mass [*Waliser et al.*, 2009] (see also Figure 1), and a reconsideration or quantification of this exclusion may be warranted.

[4] The purpose of this study is to provide the modeling community with an initial estimate of the radiative impact of these assumptions – namely ignoring precipitating ice mass. We use a cloud particle size distribution (PSD) partitioning method (W.-T. Chen et al., Partitioning CloudSat ice water content for comparison with upper-tropospheric ice in global atmospheric models, submitted to *Journal of Geophysical Research*, 2010) as a guide for distinguishing ice into two categories, larger particles considered to be precipitating hydrometeors and smaller particles considered to be quasi-suspended in clouds (Figure 1). This partitioning is broadly consistent with our earlier estimate [*Waliser et al.*, 2009] albeit with a more robust foundation. With this information, we perform calculations using a comprehensive radiative transfer scheme to obtain an estimate of the misrepresentation that might be made in a GCM calculation if the model ignores the precipitating components of the ice field. In the following sections, we introduce methodology, present the results, and discuss implications and recommendations for future research.

2. Methodology

[5] The methodology employed here is to perform a set of comprehensive atmospheric radiative transfer calculations,

[1]Jet Propulsion Laboratory, California Institute of Technology, Pasadena, California, USA.
[2]Department of Atmospheric Science, Colorado State University, Fort Collins, Colorado, USA.

0094-8276/11/2010GL046478

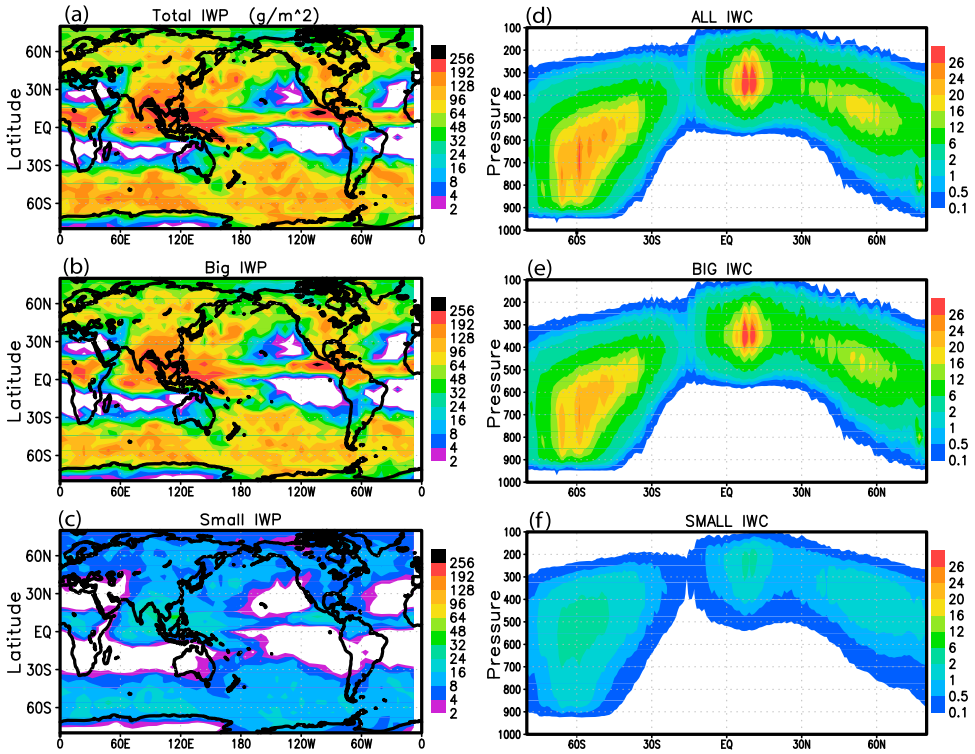

Figure 1. CloudSat estimates of mean (a) total Ice Water Path (IWP) (g m^{-2}) for July 2007. (b) An estimate of the part of Figure 1a that is associated with particle sizes (i.e., diameters of frozen spheres) greater than 100 mm. (c) Same as Figure 1b except for particle sizes less than 100 mm. (d–f) Same as Figures 1a–1c, except for zonal averages of vertically-resolved ice water content (IWC) (gm m^{-3}).

specifying as much detail from the observations as possible and including all components of the ice field. These are then contrasted with a case where an estimate of the ice mass associated with precipitation is excluded based on the PSD method (see Section 1). The radiative transfer calculations are performed using the 2B-FLXHR algorithm [*L'Ecuyer et al.*, 2008], which is a standard CloudSat retrieval product designed to produce a vertically-resolved radiative flux and heating rate dataset consistent with observed reflectivities from CloudSat's cloud profiling radar (CPR) and other satellite-observed constraints. Only the salient features are described here. Release 4 (R04) of 2B-FLXHR is based on vertical distributions of liquid and ice cloud effective radii (which typically range from 30 to several hundred microns) and water contents from the Level-2 cloud water content product (2B-CWC) [*Austin et al.*, 2009]. These cloud properties are combined with ancillary temperature and humidity profiles from the European Centre for Medium-range Weather Forecasts (ECMWF) analyses and surface albedo and emissivity data from the International Geosphere-Biosphere Programme (IGBP) global land surface classification to initialize a broadband radiative flux model known as BUGSrad. BUGSrad is based on the two-stream, doubling-adding solution to the radiative transfer equation [*Ritter and Geleyn*, 1992] and assumes a plane-parallel atmosphere over the 1.4 × 1.8 km CloudSat field of view. Rayleigh scattering, gaseous absorption, and absorption and scattering by both liquid and ice are all modeled in 2B-FLXHR. Molecular absorption and scattering properties computed using the correlated-k formulation [*Fu and Liou*, 1992] are combined with cloud optical properties based on retrieved effective radii and water contents found in CloudSat's 2B-CWC product using Mie theory for liquid particles and anomalous diffraction theory-based parameterizations for ice [*Stephens et al.*, 1990; *Mitchell et al.*, 1996]. The delta-Eddington approximation is then applied over six shortwave (SW) bands and a constant-hemisphere formulation is applied to twelve longwave (LW) bands. These bands are appropriately weighted and combined into the two broadband flux estimates that are ultimately reported, one covering the SW from 0–4 μm and the other over the LW above 4 μm. The rate of radiative heating in each layer follows simply by determining the net convergence or divergence of radiative energy into or out of it. The resulting set of SW and LW fluxes and heating rates are output for each CloudSat footprint at the maximum vertical resolution of the CPR and the 2B-CWC product, i.e., 240 m, forming the 2B-FLXHR product.

[6] Calculations are performed for the period June to August 2007. Thos including all ice represent an estimate of the "observed" radiation budget and are referred to as the "control" case. Based on comparisons against co-located Clouds and the Earth's Radiant Energy System (CERES) observations, these seasonal TOA LW and SW flux estimates at 5° resolution have uncertainties of 5 and 15 Wm^2, respectively [*L'Ecuyer et al.*, 2008]. Furthermore, these calculations do not include thin ice clouds that go undetected by CloudSat whose impact can be significant, especially in areas of persistent high thin cirrus coverage. However,

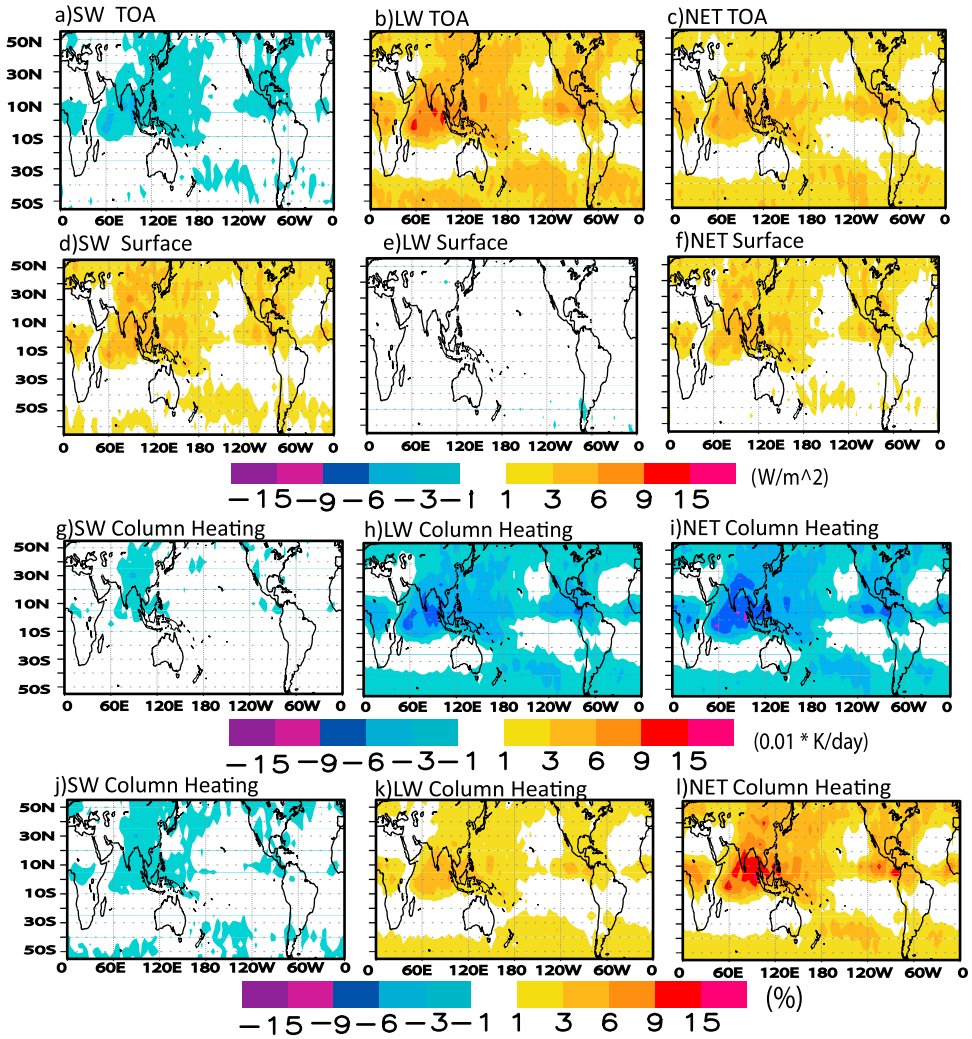

Figure 2. Differences between experiment excluding estimate of precipitation (for the case where the size threshold is 100 μm) and the control (experiment-control) for TOA (a) SW, (b) LW and (c) net radiative flux (Wm^{-2}), surface (d) SW, (e) LW and (f) net radiative flux (Wm^{-2}), (g) SW, (h) LW and (i) net column heating (K day^{-1}), and (j) SW, (k) LW and (l) net column heating (% change).

it is important to note, that a significant fraction of the absolute error that might be present in the FLXHR calculations (e.g., missing very thin cirrus) is likely to cancel in the relative differences that are the focus of this study. The "test" case consists of redoing the calculations but with an estimate of the ice mass associated with precipitation (at the 1.5 km horizontal scale of CloudSat) removed.

[7] The estimate of precipitating ice comes by utilizing the PSD parameters supplied with each CloudSat retrieval and integrating the contribution of mass above a certain size threshold - where the threshold is based on the diameter of what CloudSat assumes as frozen spherical water particles of constant density (Figure S1 of the auxiliary material).[1] In this study, we have chosen a threshold of 100 um. This is consistent with *Ryan* [2000] and nearly identical to the threshold used in the ECMWF Integrated Forecasting System (IFS) (cycles 25–31; about 2002–2006) to distinguish between cloud and precipitating ice (see www.ecmwf.int/research/ifsdocs/). Moreover, simple calculations suggest that the 100 um cutoff is representative of snowfall. Noting that the CloudSat retrieval assumes ice spheres with densities of 0.917 g cm^{-3}, an ice particle with a diameter of 100 um has a mass of 4.8×10^{-7} g. Following the planer polycrystal model of *Mitchell* [1996], this is equivalent to an aggregate with a maximum dimension of ~200 um that will fall at ~30 cm s^{-1} [*Mitchell and Heymsfield*, 2005] (assuming 220 hPa and 230 K). Thus while the 100 um threshold was chosen based primarily on model considerations, it is also physically consistent with precipitating ice particles. However, as there is still considerable leeway in how to distinguish between cloud and precipitating ice in models or observations, we have performed calculations for three different thresholds, 75, 100 and 150 μm. For a given threshold, a revised effective radius for the radiation calculations is computed from the remaining (small size) part of the distribution (Figure S2). Keep in mind

[1]Auxiliary materials are available in the HTML. doi:10.1029/2010GL046478.

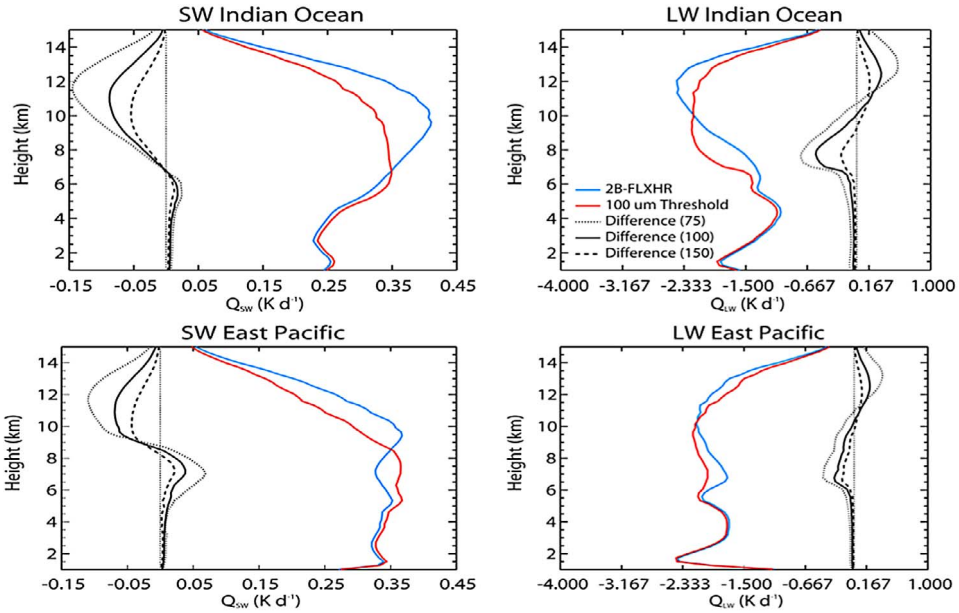

Figure 3. (left) Shortwave and (right) longwave atmospheric radiative heating profiles for the control (blue), test (red) and their difference (black) give a size threshold of 100 μm for (top) a region in the Indian Ocean (55–105 E; 5S–10N) and (bottom) a region in the eastern Pacific Ocean (75–135W; 0–15N). Dashed and dotted black lines show sensitivity of the differences to size thresholds of 150 and 75 μm, respectively.

that while the magnitude of the ice mass removed is large, it is associated with much larger particles with a significantly smaller number concentration and thus has less impact on radiation – which is why such components have been typically ignored. For both the control and test cases, the model calculations are gridded to 5° horizontal resolution to improve sampling.

3. Results

[8] Comparing the results from the control case, that is an estimate of the observed radiation budget using the total amount of ice, to the test case that is an estimate of the radiation budget if ice associated with precipitation is ignored, indicates the impact from the latter may be important in light of the level of refinements the cloud-radiation community are making at this stage of model development and with respect to the size of anthropogenic radiative forcings associated with greenhouse gases and aerosols. Figure 2 shows the differences (experiment minus control) in shortwave and longwave fluxes at the surface and top of the atmosphere in Wm^{-2} and column-integrated radiative heating expressed in terms °K day^{-1} and % change. The calculations show that omitting the precipitating ice increases the net heating at the surface and the cooling to space, each by up to about 5 Wm^{-2} in the tropical regions with the heaviest rainfall. The excess heating at the surface is dominated by changes in shortwave radiation, with little impact from the longwave as its surface signature is dominated at the by lower-atmosphere water vapor and low clouds, neither of which was altered in this experiment. The excess cooling to space has contributions from both the reduced reflection of shortwave and enhanced longwave emission, with the latter dominating. Column radiative cooling is enhanced by about 10% in the absence of precipitating ice, amounting to an excess column cooling of about 0.1 °K day^{-1}.

[9] The vertical structure of shortwave and longwave atmospheric radiative heating, and their changes, are shown in Figure 3 for two regions where the impacts of the experiment are most evident. In the shortwave, the removal of precipitating ice reduces the absorption in the upper troposphere at the ice cloud level and above. The removal of ice in the upper troposphere thus diminishes absorption within ice clouds and reduces the amount of shortwave radiation that is absorbed by water vapor and ozone above the cloud layer (i.e., >~12 km) by reducing reflection back to space. This occurs similarly for both the Indian Ocean and Eastern Pacific region illustrated. Below the ice cloud layer, the removal of precipitating ice leads to slightly enhanced absorption of shortwave radiation as there is now more passing through the upper ice cloud layer available for absorption below. In the longwave, the removal of the precipitating cloud ice produces a heating-cooling couplet by lowering the average effective atmospheric emission level. Reducing ice mass allows longwave radiation to penetrate deeper into ice clouds resulting in a broadening of the aggregated cloud top cooling layer in each region. The middle-upper troposphere, therefore, emits more longwave and thus cools more, while above the ice cloud layer the longwave cooling is reduced (represented here as a heating). While the changes at any given altitude are only about 0.1° day^{-1}, the most important issue here is that the changes result in a modification of the vertical profile of radiative heating and thus a likely impact on the radiative component of the circulation. For considerably different thresholds for large versus small particles (e.g., 75 μm and 150 μm; Figure S3), there are still sizeable impacts on the surface and TOA net radiation, and on the

vertical distribution of heating that is shown by the dotted and dashed black curves in Figure 3.

4. Summary

[10] Climate models often do not explicitly account for the radiative impacts of ice associated precipitating hydrometeors. The justification for this typically derives from the relatively small area accounted for by precipitation at any given time and because precipitating ice hydrometeors have larger radii and smaller number concentrations than non-precipitating hydrometeors (i.e., clouds) resulting in a smaller radiative impact. Moreover, to retain the needed information for radiation calculations would often necessitate additional prognostic quantities/equations (e.g., snow, graupel) that add to the computation demands of the model. The recent availability of CloudSat estimates of atmospheric ice water content, along with the auxiliary material supplied by the retrieval on the particle size distribution (as well as supporting information on precipitation presence and cloud classification [e.g., *Waliser et al.*, 2009]) provides the means to test the potential radiative impact that precipitating hydrometeors have on the atmospheric and surface radiation budget.

[11] Using the 2B-FLXHR [*L'Ecuyer et al.*, 2008] standard output results as a control case for the radiation budget, we have performed a set of experiments that excludes the ice associated with precipitating hydrometeors. The results show that exclusion of these components of atmospheric ice can result in net surface and TOA radiative flux differences of up to 5–10 Wm^{-2} in the most convective and rainfall intensive areas, with the largest impact being on TOA emitted longwave (see Figure 2). Notable is that net column atmospheric radiative cooling increase by about 10%. More important is that the exclusion of these ice components results in changes to the structure of the longwave and shortwave radiative heating profiles, with deviations on the order of 0.1° day^{-1} and up to 10–25% (see Figure 3).

[12] When the above results are considered in the context of a climate model simulation, the changes would not only impact the radiative heating of the atmosphere but would be expected to impact the circulation, and possibly even the manner the model adjusts to external forcings such as increasing greenhouse gases. Note that the magnitude of these potential errors is on the order of the radiative heating changes associated with a doubling of atmospheric carbon dioxide. Additionally, while models are tuned to get the right TOA radiation balance, the implications here are that without considering the ice in precipitating hydrometeors explicitly the models will be getting the right result (i.e., TOA balance) for the wrong reasons. In doing so, there are likely to be compensating errors in other quantities such as cloud cover, cloud particle effective radius and/or cloud mass. Noteworthy is that recently it was shown that biases against observations in the annual average absorbed shortwave and outgoing longwave radiation across the ITCZ regions for the ensemble average of CMIP3 GCMs were found to be on the order of 25 Wm^{-2} – meaning there was too much absorbed solar and outgoing longwave radiation in the models [*Trenberth and Fasullo*, 2011]. Given that most of these models do not include the effects of ice in precipitating hydrometeors in the radiation schemes, the results of the experiment described here indicates that a part of these biases may be arising from this exclusion.

[13] The continuation of this work demands additional work with alternative methods and models for including and excluding ice associated with precipitation to test the robustness and sensitivities of the preliminary result reported here. Specifically, this study illustrates some initial calculations, based on a single season (i.e., JJA 2007) and modeling methodology, showing the possible effects of frozen precipitation on the radiation budget and radiative heating profiles, which can have a possible impact on global general circulation patterns. Further studies are needed to fine tune these results and to quantify the uncertainty due to input data sources, data sampling, and model assumptions, as well as how the effect of annual cycle of clouds and precipitation affects the current findings. Studies in the context of fully interactive GCMs are needed to understand the feedback from the coupled ocean-atmosphere-land system onto the clouds and precipitation to determine if it might contribute a negative or positive feedback on the offline calculations results presented here. In addition, complementary studies for liquid water are needed.

[14] **Acknowledgments.** We would like to thank Yuk Yung, King-Fai Li, and Lazaros Oreopoulos for reading and providing comments on the manuscript. The contributions by DEW, JLL and WTC were carried out on behalf of the Jet Propulsion Laboratory, California Institute of Technology, under a contract with the National Aeronautics and Space Administration. TSL was supported by the NASA NEWS and CloudSats projects. TSL would like to thank Phil Partain at the CloudSat Data Processing Center for assistance in running the revised FLXHR calculations.

[15] The Editor and authors thank Gerald Mace and an anonymous reviewer for their assistance in evaluating this paper.

References

Austin, R. T., A. J. Heymsfield, and G. L. Stephens (2009), Retrieval of ice cloud microphysical parameters using the CloudSat millimeter-wave radar and temperature, *J. Geophys. Res.*, *114*, D00A23, doi:10.1029/2008JD010049.

Fu, Q., and K. N. Liou (1992), On the correlated K-distribution method for radiative-transfer in nonhomogeneous atmospheres, *J. Atmos. Sci.*, *49*, 2139–2156, doi:10.1175/1520-0469(1992)049<2139:OTCDMF>2.0.CO;2.

L'Ecuyer, T. S., N. B. Wood, T. Haladay, G. L. Stephens, and P. W. Stackhouse Jr. (2008), Impact of clouds on atmospheric heating based on the R04 CloudSat fluxes and heating rates data set, *J. Geophys. Res.*, *113*, D00A15, doi:10.1029/2008JD009951.

Li, J.-F., D. E. Waliser, C. Woods, J. Teixeira, J. Bacmeister, J. Chern, B. W. Shen, A. Tompkins, and M. Kohler (2008), Comparisons of satellites liquid water estimates with ECMWF and GMAO analyses, 20th century IPCC AR4 climate simulations, and GCM simulations, *Geophys. Res. Lett.*, *35*, L19710, doi:10.1029/2008GL035427.

Mitchell, D. L. (1996), Use of mass- and area-dimensional power laws for determining precipitation particle terminal velocities, *J. Atmos. Sci.*, *53*, 1710–1723, doi:10.1175/1520-0469(1996)053<1710:UOMAAD>2.0.CO;2.

Mitchell, D. L., and A. J. Heymsfield (2005), Refinements in the treatment of ice particle terminal velocities, highlighting aggregates, *J. Atmos. Sci.*, *62*, 1637–1644, doi:10.1175/JAS3413.1.

Mitchell, D. L., A. Macke, and Y. Liu (1996), Modeling cirrus clouds. Part II: Treatment of radiative properties, *J. Atmos. Sci.*, *53*, 2967–2988, doi:10.1175/1520-0469(1996)053<2967:MCCPIT>2.0.CO;2.

Ritter, B., and J.-F. Geleyn (1992), A comprehensive radiation scheme for numerical weather prediction models with potential applications in climate simulations, *Mon. Weather Rev.*, *120*, 303–324, doi:10.1175/1520-0493(1992)120<0303:ACRSFN>2.0.CO;2.

Ryan, B. F. (2000), A bulk parameterization of the ice particle size distribution and the optical properties in ice clouds, *J. Atmos. Sci.*, *57*, 1436–1451, doi:10.1175/1520-0469(2000)057<1436:ABPOTI>2.0.CO;2.

Stephens, G. L., S. C. Tsay, P. W. Stackhouse, and P. J. Flatau (1990), The relevance of the microphysical and radiative properties of cirrus clouds

to climate and climatic feedback, *J. Atmos. Sci.*, *47*, 1742–1754, doi:10.1175/1520-0469(1990)047<1742:TROTMA>2.0.CO;2.

Stephens, G. L., et al. (2002), The CloudSat mission and the A-Train—A new dimension of space-based observations of clouds and precipitation, *Bull. Am. Meteorol. Soc.*, *83*(12), 1771–1790, doi:10.1175/BAMS-83-12-1771.

Stephens, G. L., et al. (2008), CloudSat mission: Performance and early science after the first year of operation, *J. Geophys. Res.*, *113*, D00A18, doi:10.1029/2008JD009982.

Trenberth, K. E., and J. T. Fasullo (2011), Simulation of present day and 21st century energy budgets of the southern oceans, *J. Clim.*, in press.

Waliser, D. E., et al. (2009), Cloud ice: A climate model challenge with signs and expectations of progress, *J. Geophys. Res.*, *114*, D00A21, doi:10.1029/2008JD010015.

W.-T. Chen, J.-L. F. Li, and D. E. Waliser, Jet Propulsion Laboratory, California Institute of Technology, 4800 Oak Grove Dr., Pasadena, CA 91109, USA. (duane.waliser@jpl.nasa.gov)

T. S. L'Ecuyer, Department of Atmospheric Science, Colorado State University, 1371 Campus Delivery, Fort Collins, CO 80523, USA.